

An Improved Zero Voltage/Zero Current Switching Commutation Cell for All Active Switches in a PWM DC/DC Converter

Dong-Yun Lee* and Dong-Seok Hyun*

Abstract - This paper presents an improved Zero Voltage/Zero Current Switching (ZVZCS) commutation cell with minimum additional components, which provides soft switching at both turn-on and turn-off of main and auxiliary switches as well as diodes in a PWM DC/DC converter. The proposed soft-switching technique is suitable for not only minority, but also majority carrier semiconductor devices. The auxiliary switch of the proposed ZVZCS commutation cell is in parallel with the main switch, and therefore, the main switch and the diode are free of current stress. The operation principles of the proposed ZVZCS commutation cell are theoretically analyzed using the PWM boost converter topology as an example. The validity of the PWM boost converter topology with the proposed ZVZCS commutation cell is verified through theoretical analysis, simulation and experimental results.

Keywords: Zero Voltage/Zero Current Switching (ZVZCS), minimum additional components, soft switching, commutation cell, no current stress

1. Introduction

The switching loss and noise associated with hard switching are still a problem in many applications, especially at higher operating frequencies, where the switching loss may dominate the total semiconductor loss and deteriorate the overall system efficiency.

A number of soft-switching techniques have been developed to reduce the switching losses in power devices. The classical parallel/series resonant converters, quasi-/multi-resonant converters are noticeable among them [1], [2]. However, the converters proposed in Liu and Lee's [1] and Hua and Lee's [2] studies suffer from high circulating energy and the associated high conduction loss, and need a variable frequency control of these converters to accommodate the wide load and line range.

Recently, to solve these problems, soft-switching PWM converters have been proposed such as the Zero-Voltage-Transition (ZVT) or Zero-Current-Transition (ZCT) [3]-[8], which unify the merits of both the low conduction loss associated with conventional PWM converters and the low switching loss attributed to resonant converters while avoiding their respective deficiencies.

The disadvantage of the ZVT PWM converter, however, is hard turn-off of both main and auxiliary switches. The turn-off switching loss, which is usually dominated by tail current in case of using IGBT for high power applications, cannot effectively be mitigated with the ZVT technique [3].

Power MOSFET presents better performances under ZVS/ZVT-PWM operation, since the switching loss is mainly caused by a parasitic capacitor at turn-on [9], [10].

Then, to solve this problem of ZVS/ZVT-PWM operation, ZCS/ZCT-PWM operation is more effective. However, the main switch of the ZCT PWM converter has severe current stress problem that results from circulating energy and diode reverse recovery current at turn-on [4]. To solve this disadvantage of the conventional ZCT PWM converter, variously improved ZCS commutation techniques are proposed, which maintain the advantages of the conventional ZCT PWM converter. However, both the main switch and diode still have current stress [5]-[7].

Recently, new PWM converters with only one auxiliary switch achieve simultaneously ZVS and ZCS during turn-on and turn-off of the main switch and main devices have not current stresses in [10]. In that paper, however, the rated voltage of the auxiliary switch is larger than that of the main switch, so that the utilization of the auxiliary switch deteriorates from a power point of view. Also, since the auxiliary switch is hard-switched at turn-off, MOSFET as an auxiliary switch is better than IGBT in terms of the overall system efficiency. Unfortunately, this also limits power level of the system. For higher power applications, it is necessary to solve hard turn-off and high rated voltage of the auxiliary switch.

Therefore, this paper presents an improved ZVZCS commutation cell with minimum additional components (one auxiliary switch, one resonant inductor and capacitor, and two auxiliary diodes), which provides soft switching at both turn-on and turn-off of main and auxiliary switches as

* Dept. of Electrical and Electronic Engineering, Hanyang University, Korea (dongylee00@hotmail.com, dshyun@hanyang.ac.kr)
Received August 9, 2002 ; Accepted November 15, 2002

well as diodes in PWM converters. The proposed soft-switching technique is suitable for not only minority (IGBT) but also majority carrier semiconductor devices (MOSFET). The auxiliary switch of the proposed ZVZCS commutation cell is in parallel with the main switch, and therefore, current stress on the main switch and diode is avoided. However, the voltage across the main diode during turn-on of the main switch is twice as large as the output voltage. Theoretical analysis, simulation and experimental results verify the validity of the PWM boost converter topology with the proposed ZVZCS commutation cell.

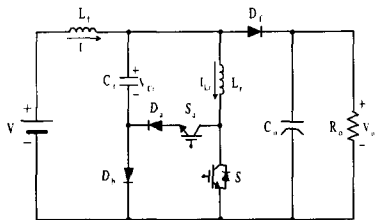
2. Theoretical Analysis

2.1 A New PWM Boost converter

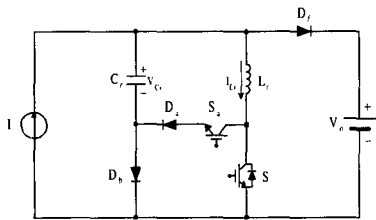
Fig. 1(a) shows the PWM boost converter with the improved soft-switching commutation cell. It differs from the conventional boost PWM converter because it possesses a resonant inductor, L_r , in series with the main switch, S , which controls di/dt of the current through it at turn-on of the auxiliary switch, S_a , a resonant capacitor, C_r , and auxiliary diodes, D_a , and D_b .

- To simplify the analysis, it is assumed that
- the converter is operating in steady-state;
- the input filter is sufficiently large to be approximated by a current source, I_i ;
- all components are ideal;
- the output voltage, V_o , is constant.

Fig. 1(b) shows the simplified circuit diagram. As shown in Fig. 2, eleven operating modes exist within one switch cycle. Fig. 3 shows the theoretical waveforms, (which are explained as follows:)



(a) The PWM boost converter with the improved soft-switching commutation cell



(b) The simplified circuit diagram

Fig. 1 The PWM boost converter diagram with the modified ZVZCS commutation cell.

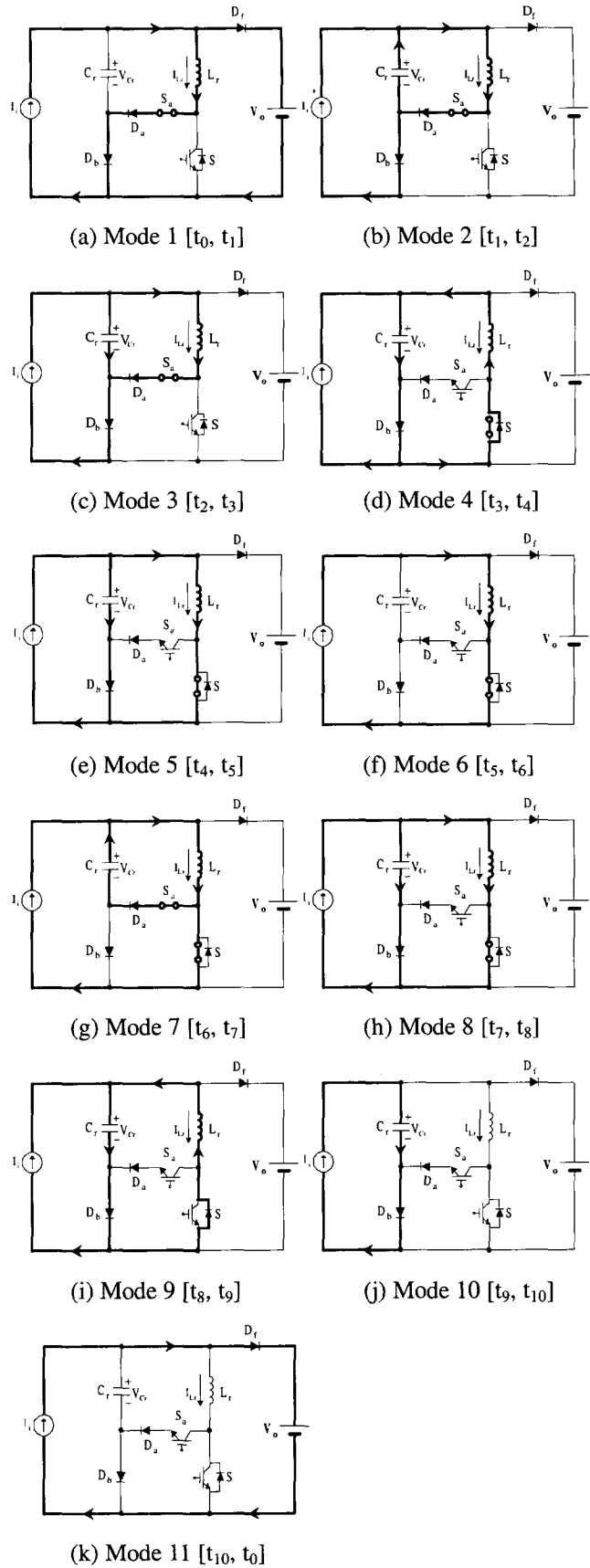


Fig. 2 Operating modes.

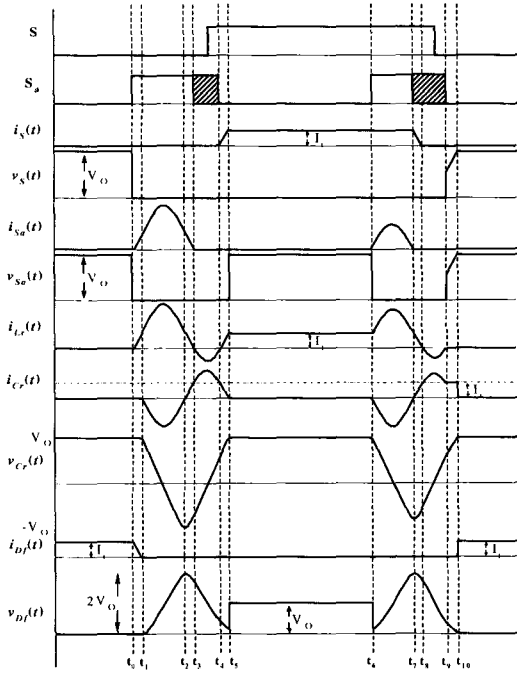


Fig. 3 Theoretical waveforms.

2.2 Operating Principles of the Proposed PWM Converter

(a) **Mode 1** [t_0 - t_1]: Prior to t_0 , both the main switch, S , and the auxiliary switch, S_a , are turned off and the input current I_i flows through the main diode, D_f . At t_0 , the auxiliary switch is turned on under ZCS. The current through the resonant inductor, L_r , increases from zero linearly until t_1 when $i_{L_r}(t) = I_i$. At the same time, the main diode current reduces linearly to zero and is turned off under ZVS. During this period, the resonant inductor current, $i_{L_r}(t)$, can be represented by

$$i_{L_r}(t) = \frac{V_o}{L_r} t \quad (1)$$

The time interval of this mode is given by

$$\Delta t_1 = \frac{I_i \cdot L_r}{V_o} \quad (2)$$

(b) **Mode 2** [t_1 - t_2]: The resonant capacitor, C_r , keeps up the output voltage, V_o , before t_1 . With the turn-off of the main diode, D_f , at t_1 , a resonance between L_r and C_r starts, which brings the auxiliary switch current to its peak value after a quarter of the resonant cycle, T_r . The resonant capacitor voltage reverses its polarity after another quarter of T_r . The resonant inductor current, $i_{L_r}(t)$, and capacitor voltage, $v_{C_r}(t)$, during this period is

$$i_{L_r}(t) = I_i + \frac{V_o}{Z_o} \sin \omega_r (t - t_1) \quad (3)$$

$$v_{C_r}(t) = V_o \cos \omega_r (t - t_1) \quad (4)$$

where, $\omega_r = 1/\sqrt{L_r \cdot C_r}$, the resonant angular frequency and $Z_o = \sqrt{L_r/C_r}$, the characteristic impedance of the resonant tanks, respectively. The time interval of this mode is given by

$$\Delta t_2 = \frac{T_r}{2} = \pi \sqrt{L_r \cdot C_r} \quad (5)$$

(c) **Mode 3** [t_2 - t_3]: At t_2 , the auxiliary switch current reaches the input current, I_i . The resonant current and the auxiliary switch current reduce from the input current until they reach zero at t_3 due to the further resonance between L_r and C_r .

(d) **Mode 4** [t_3 - t_4]: The auxiliary switch, S_a , is turned off when its current is zero at t_3 . After the same time, the voltage across the auxiliary switch maintains zero voltage by the resonance between L_r and C_r and the anti-parallel diode, D_s , of the main switch starts to conduct. During the conduction period of the diode, D_s , the main switch can be turned on under ZVS and ZCS, simultaneously. As shown in this mode, both main and auxiliary switches are commutated with no switching losses. During mode 3 and mode 4, the resonant inductor current, $i_{L_r}(t)$, and capacitor voltage, $v_{C_r}(t)$, can be expressed as follows:

$$i_{L_r}(t) = I_i - \frac{V_o}{Z_o} \sin \omega_r (t - t_4) \quad (6)$$

$$v_{C_r}(t) = -V_o \cos \omega_r (t - t_4) \quad (7)$$

The time interval of this mode is given by

$$\Delta t_{3,4} = \Delta t_3 + \Delta t_4 = \frac{T_r}{2} - \frac{T_r}{2\pi} \sin^{-1}(Z_o I_i / V_o) \quad (8)$$

where, Δt_3 and Δt_4 are the time interval of mode 3 and mode 4, respectively.

(e) **Mode 5** [t_4 - t_5]: After the commutation through the anti-parallel diode, D_s , the main switch current increases from zero to t_5 when $i_s(t) = I_i$. During this mode, the resonant inductor current, $i_{L_r}(t)$, can be represented by

$$i_{L_r}(t) = I_i - \frac{V_o}{Z_o} \sin \omega_r (t - t_5) \quad (9)$$

The time interval of this mode is given by

$$\Delta t_5 = \frac{T_r}{2\pi} \sin^{-1}(Z_o I_i / V_o) \quad (10)$$

(f) Mode 6 [t₅-t₆]: The operation of the circuit at this mode is similar to the turn-on state of the conventional PWM boost converter. The input current, I_i , flows through $L_f \rightarrow L_r \rightarrow S$. During this mode, the auxiliary switch, S_a , holds V_o .

(g) Mode 7 [t₆-t₇]: At t_6 , the auxiliary switch, S_a , is turned on under ZCS by the resonance between L_r and C_r . During this mode, the resonant inductor current, $i_{L_r}(t)$, and capacitor voltage, $v_{C_r}(t)$, can be represented by

$$i_{L_r}(t) = I_i + \frac{V_o}{Z_o} \sin \omega_r (t - t_7) \quad (11)$$

$$v_{C_r}(t) = V_o \cos \omega_r (t - t_7) \quad (12)$$

The duration of the resonance is given by

$$\Delta t_7 = T_r / 2 = \pi \sqrt{L_r \cdot C_r} = \Delta t_2 \quad (13)$$

(h) Mode 8 [t₇-t₈]: The auxiliary switch, S_a , is turned off after $T_r/2$. After t_7 , the voltage across S_a maintains zero voltage by further resonance between L_r and C_r , and therefore, the auxiliary switch achieves perfect zero-voltage-switching. The current through L_r and S is brought down to zero at t_8 .

(i) Mode 9 [t₈-t₉]: As soon as the current through L_r and S reaches zero at t_8 , the anti-parallel diode, D_s , of the main switch starts conducting. During its conduction period, the main switch can be turned off under ZCS and ZVS simultaneously. The resonance stops at t_9 , when $i_{C_r}(t) = I_i$. During this time, the resonant inductor current, $i_{L_r}(t)$, and capacitor voltage, $v_{C_r}(t)$, can be expressed as follows:

$$i_{L_r}(t) = I_i - \frac{V_o}{Z_o} \sin \omega_r (t - t_9) \quad (14)$$

$$v_{C_r}(t) = -V_o \cos \omega_r (t - t_9) \quad (15)$$

The time interval of this mode is given by

$$\Delta t_{8,9} = \Delta t_8 + \Delta t_9 = \frac{T_r}{2} - \frac{T_r}{2\pi} \sin^{-1}(Z_o I_i / V_o) \quad (16)$$

(j) Mode 10 [t₉-t₁₀]: Because the half cycle of the resonance is not completed in the previous stage, the resonant capacitor voltage at t_9 is less than V_o , as shown follows:

Using Eq.(14) and Eq. (15),

$$v_{C_r}(t_9) = V_o \sqrt{1 - (Z_o I_i / V_o)^2} < V_o \quad (17)$$

Therefore, the resonant capacitor voltage is replenished linearly to V_o by the input current I_i during t_9 to t_{10} before the main diode, D_f , can be turned on. The time interval of this mode is given by

$$\Delta t_{10} = \frac{C_r}{I_i} [V_o - V_{C_r}(t_9)] \quad (18)$$

(k) Mode 11 [t₁₀-t₀]: At t_{10} , the main diode, D_f , starts to conduct. The operation in this mode is the same as that in the conventional PWM boost converter.

At t_0 , the auxiliary switch, S_a , is turned on again, and the switching cycle is repeated from Mode 1 to Mode 11.

3. Design Guideline

3.1. Design Guideline and Example

In this section, a design procedure and an example to determine the component values of the proposed ZVZCS PWM boost converter are presented.

The initial conditions are given as follows:

- Input Voltage : $V_i = 155$ V;
- Output Voltage : $V_o = 340$ V;
- Output Power : $P_o = 1000$ W;
- Approximate efficiency : $\eta \geq 97$ %;
- Ripple of the Input Current : $\Delta i_i = 28$ %;
- Switching frequency : $f_s = 50$ kHz.

1) The input power P_i and the maximum input current I_i^{\max} can be defined by the value of the output power, the input voltage, and the approximate efficiency as follows.

$$P_i = \frac{P_o}{\eta} = 1030 \text{ W} \quad ; \quad I_i^{\max} = 1.14 \frac{P_i}{V_i} = 7.57 \text{ A}$$

2) To ensure the ZCS operation, the peak value of the resonant current during mode 9 must be larger than the maximum value of the input current I_i^{\max} .

Choosing $I_{L_{rpeak}}^{ZCS} = 15$ A, the characteristic impedance is given by

$$I_{Lrpeak}^{ZCS} > I_i^{\max} \quad ; \quad Z_1 = \frac{V_o}{I_{Crpeak}^{ZCS}} = \sqrt{\frac{L_{r1}}{C_r}} = 22.6$$

Based on a rule of thumb and through [5], the resonant frequency, f_o , was defined as about 6 times the switching frequency, f_s .

$$f_o = 5.6 f_s = 280 \text{ kHz}$$

3) With Z_o and f_o values, the resonant elements L_r and C_r , can be given. In this design example, these values are as follows:

$$L_r = 12.6 \text{ uH} \quad ; \quad C_r = 25 \text{ nF}$$

3.2 Verification through the Simulation Results

To verify the property of the proposed soft-switching commutation cell applied to the conventional PWM boost converter topology, a simulation using ideal components is performed under input voltage $V_i=155\text{V}$, output power $P_o=1\text{kW}$, switching frequency $f_s=50\text{kHz}$, and output voltage $V_o=340\text{V}$.

Fig. 4 shows the simulation waveforms. Ideally, they conform the theoretical analysis mentioned earlier in this paper.

Fig. 4(c) presents voltage and current waveforms of the main diode D_f . It can be shown that the current through the main diode D_f has no current stresses during turn-on and the diode D_f is commutated with soft switching. However, the voltage across the main diode is increased to almost two times the output voltage by the resonant capacitor voltage, and therefore, it is necessary to take into account the voltage rating in the choice of the power diode.

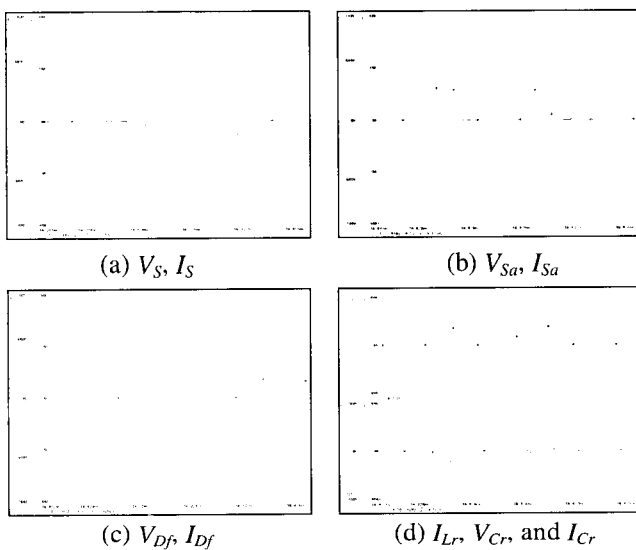


Fig. 4 Simulation waveforms.

As shown in these simulation waveforms, the merit of the proposed ZVZCS PWM converter is the ZCS operation for turn-off transitions of all the active switches in the converter, so IGBTs are a good choice for both the main and auxiliary switches. Therefore, the proposed soft-switching technique is well suited for high power applications.

4. Experimental Results

4.1 System Configuration

A 50 kHz, 1 kW prototype has been implemented. The power circuit components and their specifications are shown in Fig. 5 and Table I.

The main switch and the auxiliary switch are implemented with a high speed IGBT, (SEC) SGH30N60RUFD (600V, 30A).

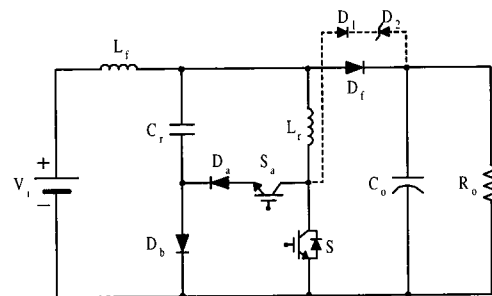


Fig. 5 Power circuit configuration.

Table 1 Experimental parameters.

S	SGH30N60RUFD	Sa	SGH30N60RUFD
D	DSEI30-10A	Lr	12.6uH(TDK PC40EI40-Z)
Da	ESAC92M-02	Lf	990uH(TDK PC40EI60-Z)
Db, D1	DSEI30-06A	Cr	25nF
D2	1N5337B	Co	330uF
Vi	155V	Po	1kW

The auxiliary diode, D_b , is fast recovery epitaxial diode (IXYS) DSEI30-06A (600V, 30A). To reduce the ringing between L_r , C_r and the output capacitance of the auxiliary switch, S_a , the additional diode, D_a , was used. The auxiliary diode used as D_a is an ultra fast recovery diode (FUSI) ESAC92M-02 (200V, 10A). The freewheeling diode used is a 1000 V fast recovery epitaxial diode, DSEI30-10A, because it has to sustain voltage twice as high as the output voltage, i.e. 780 V by the resonance of the auxiliary circuit.

4.2 Results and Analysis

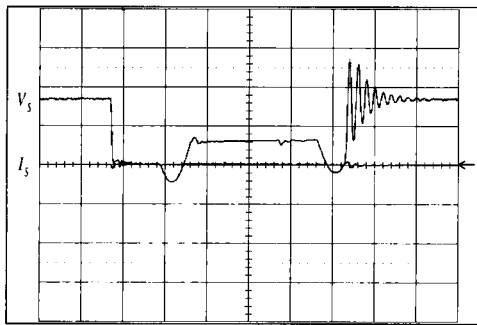
Fig. 6 shows the experimental waveform of the main switch without a clamping circuit.

As shown in this waveform, however, the switch voltage

will be ringing due to the oscillation between L_r and the output capacitor of the switch after the switch is turned off, although the switch is operated by ZCS.

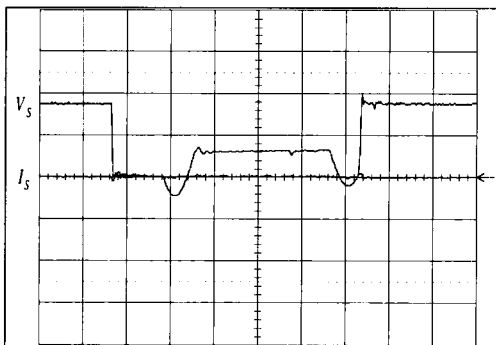
Usually in converter designs, the common sense is to minimize the wiring and connection inductance in order to minimize the switch voltage overshoot. However, in this proposed converter, the main switch voltage suffers from ringing and overshoot because of the existence of the resonant inductor, L_r , into the main power path. So, the switch voltage must be clamped somehow [5].

Fortunately, the best method for clearing this problem was presented in the reference [5]. The switch voltage is clamped to a voltage slightly higher than the output voltage, and a low voltage zener diode in series with the clamp diode furnishes this function perfectly, as shown by the dashed lines in Fig. 5.

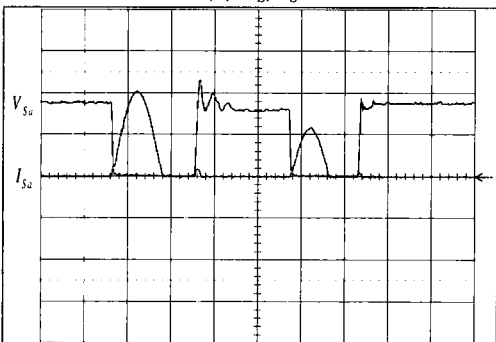


(V_s : 200 V/div., I_s : 10 A/div., Time: 2 us/div.)

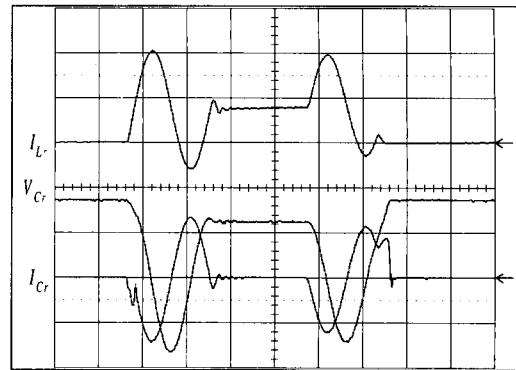
Fig. 6 The experimental waveforms of the main switch without the clamping circuit.



(a) V_s, I_s



(b) V_{Sa}, I_{Sa}



(c) I_{Lr}, V_{Cr} and I_{Cr}

(V_s, V_{Sa}, V_{Cr} : 200 V/div., $I_s, I_{Sa}, I_{Lr}, I_{Cr}$: 10 A/div., Time: 2 us/div.)

Fig. 7 The experimental waveforms of the proposed ZVZCS PWM converter with the clamping circuit.

Fig. 7 shows the experimental waveforms, which are performed by using the clamping method of the reference [5].

Actually, the experimental waveforms are identical to the theoretical analysis above mentioned with the exception the voltage waveform of the resonant capacitor, C_r . At the end of Mode 5, the charged voltage across the resonant capacitor was lower than the output voltage. As shown in Fig. 7(a), the main switch, S , is commutated without loss under ZVS and ZCS simultaneously and the switch current has no current stresses during turn-on of the main switch. These are very interesting features of the proposed soft-switching technique.

Fig. 7(b) shows that the auxiliary switch, S_a , is turned on under ZCS by existing the resonant inductor, L_r , which controls di/dt of the current of both main and auxiliary switches and eliminates the reverse recovery current of the main diode, D_f . The auxiliary switch is turned off under ZCS and ZVS perfectly. Although the auxiliary switch current waveform exhibits a resonant peak value, it does not significantly increase the conduction loss, since the resonant transition time is very short with respect to the switching cycle. Fig. 7(c) shows the voltage waveform of resonant capacitor, C_r , and the current waveform of the resonant inductors, L_r . From the waveforms, we know that the experimental results are in good accordance with the simulation results.

Fig. 8 shows the trajectories of the voltage and current of the main switch for the switching transitions. Certainly, these pictures show that the proposed PWM converter is superior to the conventional hard-switched converter.

Fig. 9 shows the efficiency curve of the proposed PWM boost converter. It is seen that the efficiency of this topology is about 97.5 % at full load. However, when the load level is decreased, the efficiency drops. This is the reason why the commutation energy is almost constant regardless of the load levels.

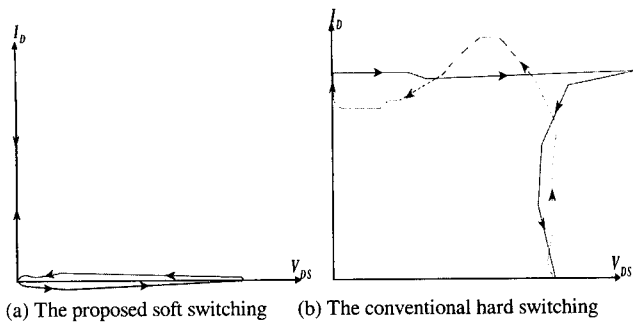


Fig. 8 Transition trajectories.

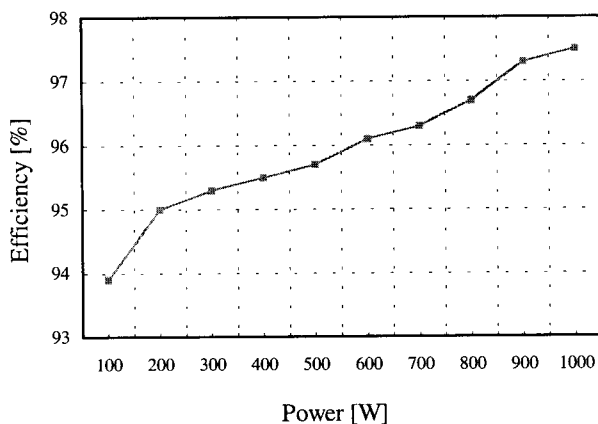


Fig. 9 The measured efficiency curve.

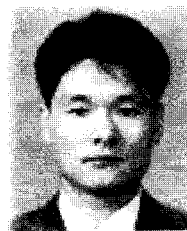
5. Conclusion

An improved ZVZCS PWM DC/DC boost converter topology has been presented. The experimental results confirm the validity of this new converter. As a conclusion, the following features can be referred to this converter:

- All active switches (S , S_a) and diodes (D_f , D_a , D_b) can be commutated under ZVS and ZCS simultaneously at turn on and turn-off. This proposed converter is especially well suited for high power applications, where IGBTs can be used as all the active switches.
- The main switch and diode have no current stresses.
- This proposed technique is suitable for minority as well as majority carrier semiconductor devices.
- Soft-switching operation can be easily maintained for a wide range of load.

References

- [1] K. H. Liu and F. C. Lee., "Zero-Voltage Switching Technique in DC-DC Converters," in *IEEE Trans. on Power Electronics.*, Vol. 5, No. 3, pp. 293-304, July 1990.
- [2] G. Hua and F. C. Lee., "Soft-Switching Technique in PWM Converter," *IEEE IECON'93.*, Vol. 2, No. 2, pp. 637-643.
- [3] G. Hua, C. Leu, and F. C. Lee., "Novel Zero-Voltage-Transition PWM Converters", *IEEE Trans. on Power Electronics.*, Vol. 9, No 2, pp. 213-219, March 1994.
- [4] G. Hua, X. Yang, Y. Jiang, and F. C. Lee., "Novel Zero-Current-Transition PWM Converters", *IEEE Trans. on Power Electronics.*, Vol. 9, No 6, pp. 601-606, Nov. 1994.
- [5] K. Wang, G. Hua, and F. C. Lee., "Analysis, Design and Experimental Results of ZCS-PWM Boost Converters," *IEEJ IPEC. Record.*, pp. 1197-1202, 1995.
- [6] H. Mao, F. C. Lee, X. Zhou, and Dushan Boroyevich., "Improved ZCT Converters for High Power Application," *Proceeding of IEEE IAS.*, pp. 1145-1152, 1996.
- [7] R. L. Lin, F. C. Lee., "Novel Zero-Voltage-Switching-Zero-Current-Switching Converters," *IEEE Power Electronics Specialists Conf. Rec.*, pp. 438-442, 1996.
- [8] R. C. Fuentes and H. L. Hey., "An Improved ZCS-PWM Commutation Cell for IGBT's Application", *IEEE Trans. on Power Electronics.*, Vol. 14, No. 5, pp. 939-948, Sept. 1999.
- [9] K. Wang, F. C. Lee, G. Hua, and D. Borojevic, "A Comparative Study of Switching Losses of IGBT's under Hard-Switching, Zero-Voltage-Switching and Zero-Current-Switching," *IEEE Power Electronics Specialists Conf. Rec.*, pp. 1196-1204, 1994.
- [10] S. H. Ryu, D. Y. Lee, S. B. Yoo, and D. S. Hyun., "New ZVZCS PWM DC-DC Converters With One Auxiliary Switch," *IEEE Power Electronics Specialists Conf. Rec.*, pp. 445-450, 1999.



Dong-Yun Lee

He was born in Chonbuk, Korea, in 1968. He received the M.S. degree in electrical engineering in 1998 from Hanyang University, Seoul, Korea, where he is currently working toward the Ph.D. degree. Since 1998, he has been with Korea Institute of Science and Technology (KIST), Seoul, Korea, as a researcher.

His primary areas of research interest include high-frequency resonant inverter, high frequency PWM DC-DC converter topology and its control circuit, soft switching techniques such as ZVS, ZCS, power factor correction circuits, and electronic ballast.

**Dong-Seok Hyun**

He received the B.E. and M.E. degrees in electrical engineering from Hanyang University, Seoul, Korea, in 1973 and 1978, respectively, and the Ph.D. degree in electrical engineering from Seoul National University, Seoul, Korea, in 1986.

From 1976 to 1979, he was with the Agency of Defense Development, Korea, as a researcher. He was a Research Associate in the department of Electrical Engineering, University of Toledo, Toledo, OH, during 1984-1985, and a visiting professor in of Electrical Engineering at the Technical University of Munich, Germany, during 1988-1989. Since 1979, he has been with Hanyang University, where he is currently a Professor in the Department of Electrical Engineering and Director of the Advanced Institute of Electrical Engineering and Electronics (AIEE). He is the author of more than 80 publications concerning electric machine design, high-power engineering, power electronics, and motor drives. His research interests include power electronics, digital signal processing, traction, and their control systems.

Dr. Hyun is a member of the IEEE Power Electronics, IEEE Industrial Electronics, IEEE Industry Applications, and IEEE Electron Devices Societies, the Institution of Electrical Engineers (U.K.), the Korea Institute of Electrical Engineers, and the Circuit Control Society.